Chemical Engineering Science xxx (xxxx) 119618

Contents lists available at ScienceDirect

Chemical Engineering Science

journal homepage: www.elsevier.com

CO_2 capture and utilization by biocatalytic synthesis of carboxylic acids: a process design study

Luigi Marra [a], Maria Elena Russo [b], Hanna K. Knuutila [c], Antonio Marzocchella [a], Piero Salatino [a]

[a] Dipartimento di Ingegneria Chimica, dei Materiali e della Produzione Industriale, Università degli Studi di Napoli Federico II, Napoli, Italy
[b] Istituto di Scienze e Tecnologie per l'Energia e la Mobilità Sostenibili, Consiglio Nazionale delle Ricerche - CNR, Napoli, Italy
[c] Department of Chemical Engineering, Norwegian University of Science and Technology, N-7491 Trondheim, Norway

ARTICLE INFO

Keywords:
CO_2 capture
CO_2 utilization
Carbonic anhydrase
Decarboxylase
Absorption
Carboxylic acids

ABSTRACT

The search for less energy-intensive processes is pushing toward a diversification of Carbon-Capture and Utilization/Sequestration (CCU/S) pathways. Biocatalytic processes offer sustainable solutions characterized by extremely mild operating conditions. Over the last decade, post-combustion CO_2 capture based on enzymatic reactive absorption experienced remarkable growth from the laboratory to the demonstration scale. The present study explores a novel CCU concept based on phenol carboxylation catalyzed by cofactor-free decarboxylases. The design of the CCU process includes CO_2 capture by alkaline solvents boosted by carbonic anhydrase followed by bicarbonate fixation via enzymatic phenol carboxylation. Phenols generated from fractional pyrolysis of biomass were assumed as carboxylation substrates. Two process layouts have been developed and modelled, and reliable experimental data and kinetic model supported the computations. Simulated best cases prove to be feasible options for integrating the enzyme cascade with the conventional CO_2 absorption/desorption loop and lignocellulose biomass-derived substrates.

1. Introduction

Mitigation of climate change encompasses a wide set of measures. Among these, reducing greenhouse gas emissions through CO_2 capture from point sources (mainly power plants and hard-to-abate industrial processes) followed by storage and/or utilization processes plays a significant role. Indeed, CO_2 may be a valuable component in several industrial applications as well as a substrate in biotechnological processes. Enzymes and microorganisms able to convert and fix CO_2 into valuable products or intermediates are gaining interest, e.g. in methane synthesis through bio-electrochemical anaerobic digestion (Wang et al., 2023) and biodiesel production through microalgae or cyanobacteria (Severo et al., 2019, Dineshkumar et al., 2015). Moreover, the significant energy penalty affecting the costs of CO_2 capture (Ember, 2022) is driving researchers to search for less energy-intensive, more economical capture paths as one key to CCU/S feasibility. Post-combustion CO_2 capture by cyclic absorption/desorption is accomplished by absorption of CO_2 in alkaline solvents (Liu et al., 2020, De Carvalho Pinto et al., 2022, Borhani et al., 2015), followed by recovery of concentrated CO_2 using a thermal stripping column (Knuutila et al., 2009). This process is most typically carried out with amine-based solvents, but recently also carbonate/bicarbonate solutions with enzymatic promoters have been successfully proposed. The use of amine-free solutions allows for capture of CO_2 in bicarbonate solutions (wet capture) and, therefore, opens the path toward direct conversion of bicarbonate into products, which may represent a less energy-intensive solution to CO_2 utilization.

1.1. CO_2 reactive absorption in carbonate/bicarbonate solutions

Fig. 1 reports a typical post-combustion CO_2 capture process based on reactive absorption followed by continuous thermal desorption where the CO_2-rich solution produced in the absorption unit is thermally regenerated in a stripping unit. The required heat for the desorption process is supplied to the reboiler typically by using low-temperature steam available in the power plant. Energy integration is accomplished by pre-heating the solution by exploiting the enthalpy of the CO_2 lean solution recirculated to the absorption column. The stream of concentrated CO_2 is recovered and separated from water vapor by condensation downstream of the stripper.

The environmentally friendly and non-volatile nature and the thermal stability of sodium and potassium carbonate solutions make them promising and effective solvents for CO_2 wet capture. The substantial absence of solvent emissions and the non-degradable nature of the solvent drastically reduce the ancillary costs typically associated with amines' oxidative and thermal degradation. As a drawback, carbonates-based solvents have low CO_2 absorption rates (Harte and Baker, 1933; Comstock and Dodge, 1937; Knuutila et al., 2010), and absorption promoters must be added to make the process competitive compared to the amine-based options. Several inorganic promoters have been studied

https://doi.org/10.1016/j.ces.2023.119618
Received 3 August 2023; Received in revised form 3 November 2023; Accepted 4 December 2023
0009-2509/

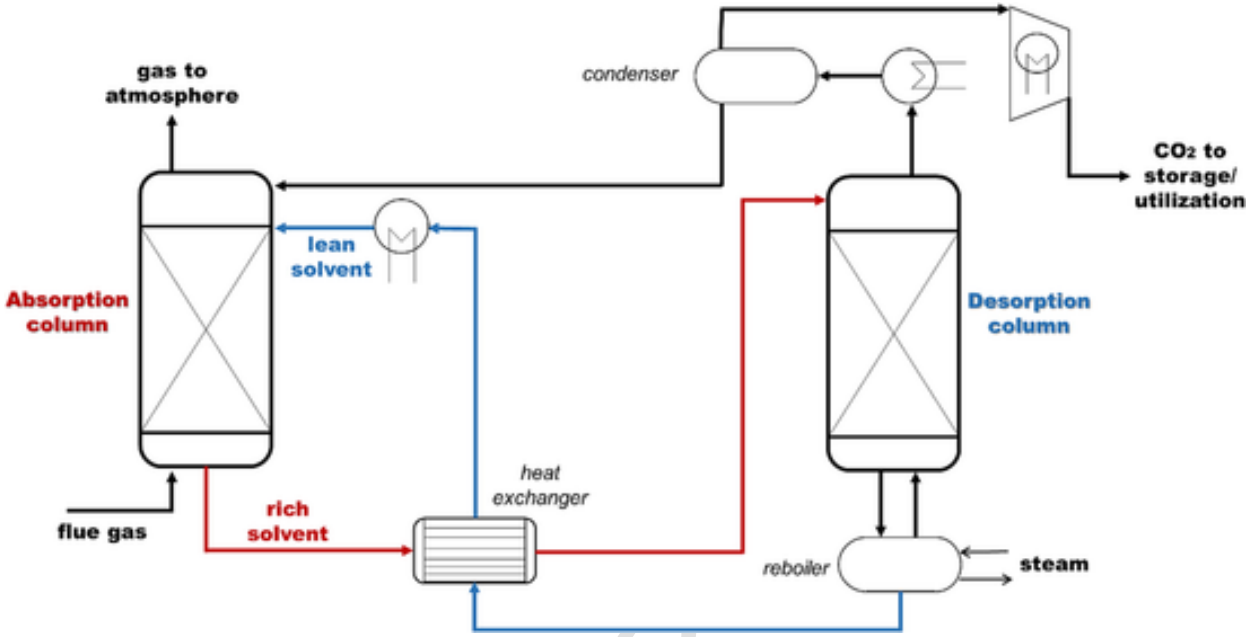

Fig. 1. Typical layout of an absorption-based CO_2 capture process (Russo et al., 2022).

over the years. The best-performing inorganic promoter is arsenic acid, but it cannot be considered as a feasible solution for industrial-scale applications due to its toxicity (Hu et al., 2016). Another widely studied option is the addition of a fast-reacting amine to promote absorption (Hu et al., 2016). However, adding amines will imply that amine emission mitigation systems will be needed, and amine degradation will also require additional solvent management strategies. A less problematic promoter for carbonate-based solvents is represented by the enzyme carbonic anhydrase .

1.2. CO_2 reactive absorption in bicarbonate/carbonate solutions promoted by carbonic anhydrase

Carbonic anhydrase (CA) (EC 4.2.1.1) catalyzes the reaction of CO_2 hydration (Eq. (1)) and thus increases the overall rate of CO_2 reactive absorption in aqueous solutions. The spontaneous uncatalyzed CO_2 hydration reaction contributes to a very limited extent to the overall absorption rate in alkaline solutions (pH > 8), because the overall absorption rate is mostly affected by the rate of CO_2 hydroxylation reaction (Eq. (2)).

$$CO_{2(liq)} + H_2O \overset{CA}{\leftrightarrow} HCO_3^- + H^+ \quad (1)$$

$$CO_{2(liq)} + OH^- \leftrightarrow HCO_3^- \quad (2)$$

In carbonate solutions, carbonate ions accept the protons released from CO_2 hydration, forming a further bicarbonate ion (Eq. (3)). Equation (4) is the resulting overall reaction occurring in alkaline carbonate solutions along CO_2 reactive absorption.

$$CO_3^{2-} + H^+ \leftrightarrow HCO_3^- \quad (3)$$

$$CO_{2(liq)} + CO_3^{2-} + H_2O \leftrightarrow 2HCO_3^- \quad (4)$$

Several CAs have been studied and characterized in alkaline solutions (pH > 8), and several authors demonstrated their stability up to 40–50 °C and resistance to some pollutants (SO_2, NO_X) of flue gas (Russo et al., 2013a). The effectiveness of CA is maximized by its presence in proximity of the gas–liquid contact surface. To this aim, technical solutions for both CA immobilization and gas–liquid contactors, such as packed columns (Russo et al., 2016, Reardon et al., 2014) or membrane reactors (Rasouli et al., 2021), have been purposely designed and developed. Free CAs have been studied and tested at both laboratory and pilot scales (Peirce et al., 2018a; Kunze et al., 2015). Despite some thermostable CA forms being active and stable even as free enzymes, the high temperature in the stripping column can inactivate them. This would require enzyme recovery prior to stripping, which may be extremely cumbersome and expensive. Successful immobilization of CA (Russo et al., 2022) on dispersed solid particles through covalent attachment, physical adsorption, or matrix entrapment results in a more stable catalyst that can be confined inside the absorption unit and can be easily recovered (Xu et al., 2021; Shamna et al., 2021; Liu et al., 2018). Moreover, much larger enzyme loadings are permitted by immobilization, avoiding protein precipitation and foaming in high carbonate concentration solvents (Peirce et al., 2018a).

1.3. Wet capture and biotechnological routes for CO_2 utilization

Wet capture provides CO_2 as bicarbonate ions that can be used as C1 source for several biotechnological applications. Seawater microalgae are commonly cultivated using culture media where the carbon source is potassium or sodium bicarbonate. The use of bicarbonate instead of CO_2-enriched air fed to photobioreactors where microbial growth occurs is a promising strategy to maximize CO_2 bio-fixation, reducing CO_2 losses to the atmosphere and avoiding some pollutants contamination that can inhibit the growth (Jun et al., 2020; Song et al., 2019).

Besides this microbial use of bicarbonate as a carbon vector towards CO_2 utilization, other enzyme-catalyzed bioprocesses require aqueous sources of CO_2/HCO_3^-. The cell-free synthesis of high-valued phenolic acids from phenolic compounds (catechol, orcinol, resorcinol) and CO_2/HCO_3^- was proved using co-factor free decarboxylases (Aresta et al., 1998; Yoshida et al., 2004; Wuensch et al., 2014). This process can be considered a novel biocatalytic pathway for CCU made possible by electron-rich co-substrates (phenols) and enzymatic carboxylation. Indeed, in the biological equivalent of Kolbe-Schmitt reaction (Lindsey and Jeskey, 1957), an electron-rich substrate (phenols) reacts with a bicarbonate ion to form a more polar carboxylate anion (Payer et al., 2019). This type of reaction is catalyzed by cofactor-free and non-oxidative dihydroxy-benzoic acid (de)carboxylases (DCs) that bind one bicarbonate ion to the aromatic ring, releasing a water molecule (Glueck et al., 2010; Tommasi, 2019). These enzymes catalyze the de-

carboxylation reaction in the metabolisms of fungi and bacteria, and the reversible nature of this reaction makes it suitable for CCU-directed biotechnological carboxylation of phenols, illustrated in Fig. 2 with reference to catechol and orcinol.

Phenol carboxylation promoted by DC occurs at mild temperatures (30 °C) and shows high regioselectivities towards *ortho*-carboxylated products, which avoid side product synthesis, unlike the conventional Kolbe-Schmitt reaction. These carboxylic acids have a large market as intermediate components for the synthesis of biopolymers, coatings, active pharmaceutical ingredients and food additives.

Lab-scale carboxylation tests have been carried out for catechol (Pesci et al., 2015), orcinol (Meyer et al., 2018) and resorcinol (Ohde et al., 2021) using free DCs as a biocatalyst. Pesci et al. (2015) investigated the kinetics of the reversible carboxylation of catechol including the effect of bicarbonate as the co-substrate , that was correlated according to a Michaelis-Menten model. An extensive screening of phenolic substrates has been reported by Wuensch et al. (2014). Results show the effect of the excess bicarbonate ions and the phenol concentration on the theoretical phenol conversion degree. Bicarbonate concentration showed the most evident effect on conversion degree: 1.5–2 M HCO_3^- is necessary to achieve the maximum theoretical phenol conversion (between 20 and 50 %). Phenol concentrations larger than 80–100 mM lead to possible enzyme deactivation and a critical drop in the conversion. The solubility of phenolic compounds in carbonate/bicarbonate solutions may be a further constraint. To overcome thermodynamic limitations, several product separation protocols have been proposed. Ohde et al., (2021) showed how adding quaternary amines for *in situ* carboxylic acid precipitation can improve the yield by pushing the equilibrium reaction towards carboxylic acids. Meyer et al. (2018) proposed using ion-exchange resins (IERs) and nonionic adsorbents to remove both orcinol and the produced 2,6-dihydroxy-4-methylbenzoic acid. Anionic IERs (cloride form), such as Dowex 1x2 and Diaion PA312, showed a good affinity towards both molecules and completely removed them in about 30 min in 2.5 M potassium bicarbonate solution in a stirred tank vessel. The use of IERs is strictly related to the pH in the reaction volume since both orcinol and the carboxylic acids can be present or not as dissociated species. Between pH 9 and 11, orcinol is mostly mono-dissociated and so it is easily removed by the anionic IER. However, this essential feature is not highlighted in the other previously mentioned studies. Moreover, although these product recovery solutions are promising, accumulation of amines or released ions from IER must be considered when solvent regeneration and reuse are considered. Hence, carboxylic acid removal from alkaline solutions at large HCO_3^- concentrations and solvent regeneration stem out as two aspects of primary importance for cyclic CCU potential applications.

The large excess of bicarbonate (>1.5 M) necessary to boost carboxylation suggests a possible exploitation of the rich solvent from CO_2 reactive absorption units. A sustainable source of electron-rich substrates (low molecular weight aromatics) is represented by bio-based phenols. Accordingly, the interesting perspective of bridging the bioconversion pathway with pyrolytic conversion of lignocellulosic biomass in the light of modern biorefinery views (Luque et al., 2014; Fonts et al., 2021; Brown, 2021) has been pursued by assuming pyrolytic phenols from fractional pyrolysis of biomass as carboxylation substrates. Combining bio-based (phenols) and CO_2-based (bicarbonate) building blocks offers a promising pathway to approach net zero emission by integrating lignocellulosic biomass waste valorization and CCU.

In a previous preliminary study, enzymatic reactive absorption (ERA) of CO_2 and enzymatic carboxylation (EC) were modelled based on (de)carboxylation equilibrium and mass balances (Marra et al., 2022). The study showed that large bicarbonate concentrations (about 2 M) increase phenol equilibrium conversion for both catechol and orcinol as substrates. However, phenol concentration affects the equilibrium conversion in the range of 50–80 mM to a limited extent. Moreover, orcinol's higher equilibrium constant resulted in a higher equilibrium conversion. As expected, based on chemical/physical data, phenols concentration is the tighter limit due to 1:1 EC stoichiometry. In addition, the phenols' solubility limits the amount of CO_2 converted to carboxylic acid, and, DC deactivation limits the maximum phenol concentrations (Pesci et al., 2015). DC immobilization can be a promising tool to increase protein resistance to phenols, but to our knowledge, no studies about DC immobilization have been reported yet. Some alternative solvents, including ionic liquid and deep eutectic solvents (DES), have been proposed for CO_2 capture (Sarmad et al., 2017; He et al., 2023) and may help to overcome limitations posed by phenols solubility, e.g. in phenols extraction from pyrolytic bio-oil by DES (Hizaddin et al., 2022).

Enzymatic carboxylation of phenols is the focus of the present study, with the aim of scrutinizing the feasibility of an attractive pathway for CO_2 utilization in industrial decarbonization. Using biobased phenols derived from fast pyrolysis of biomass as the carboxylation substrates establishes a promising bridge between bioprocess engineering and thermochemical conversion of biomass. Process engineering is undertaken by proper consideration of thermodynamic constraints and the performances of EC reactions (Payer et al., 2019). Two scenarios are analyzed. In the first scenario (Layout 1), a CO_2 capture plant is entirely dedicated to carbon fixation via carboxylation through the reaction of

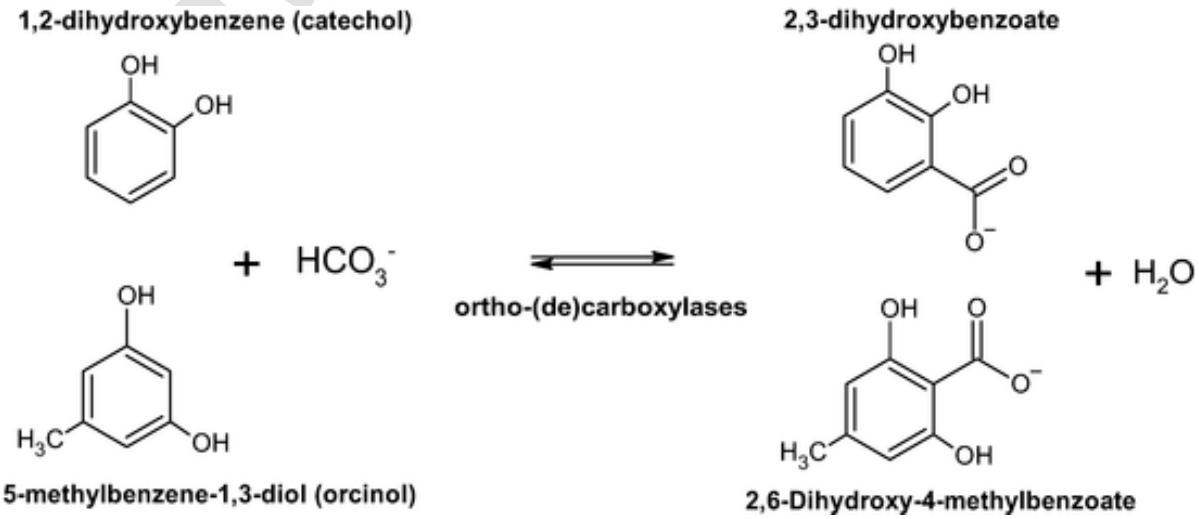

Fig. 2. Reversible enzymatic carboxylation of catechol and orcinol.

the bicarbonate intermediate with a phenolic feedstock supplied via a bio-oil extended supply chain. This scenario is consistent with a vision based on decentralized pyrolysis of raw biomass and generation of bio-oil at satellite biomass harvesting/collection sites, which then feeds into larger centralized processing or upgrading biorefineries (Kang et al., 2021; Troiano et al., 2022). A second scenario (Layout 2) assumes a CO_2 ERA-based closed-loop process, whence a fraction of the bicarbonate intermediate is used for the carboxylation of phenols generated by a dedicated medium-sized pyrolysis plant. The two layouts represent different realistic contexts and are characterized by different optimization criteria. Both configurations were modelled using ASPEN PLUS® with custom-based kinetics of the relevant reactions. The EC unit was developed considering alternative reactor configurations (packed bed and series of stirred reactors) depending on the type of biocatalysts (DC covalently immobilized on solid particles and cross-linked enzyme aggregates, respectively). Catechol and orcinol were set as reference substrates in both layouts' simulations.

2. Methods

2.1. General features of the model

The process model was developed considering two layouts, both embodying a CO_2 ERA stage and an EC stage.

Layout 1 aims at the fixation of the whole stream of captured CO_2 into carboxylic acids. The process layout (Fig. 3) takes as an input the flue gas from an industrial point source (e.g. a power plant) to be treated in the ERA unit with an enzymatically promoted potassium carbonate solution. The EC unit is continuously fed with the bicarbonate-rich solvent from the CO_2 ERA unit. The phenols stream is fed according to a distributed pattern to each EC reactor to keep phenol concentration below the solubility limit (50–80 mM) at any stage of the process. Assuming complete separation/recovery of the carboxylic acids, the bicarbonate/carbonate solvent is recycled back to the ERA CO_2 unit. The CO_2 ERA unit was designed according to Marra et al. (2022) to meet the bicarbonate excess demand of the EC process (see section 3.2).

Unlike the previous scheme, Layout 2 (Fig. 4) corresponds to a 'conventional' absorption–desorption process for CO_2 capture, whereby only a portion of the rich solvent is treated in the EC section, depending on the available stream of phenolic substrates. The CO_2 not converted to carboxylic acids is recovered in the desorber as a gas stream and compressed for further utilization or storage. Phenols are mixed with the rich solvent fraction before entering the first EC subunit to achieve the desired inlet phenol concentration (50–80 mM). Assuming a complete separation/recovery of carboxylic acids, the potassium bicarbonate/carbonate solvent from the EC unit is combined with the rich solvent stream from the CO_2 ERA unit and fed to the CO_2 desorption column to recover CO_2 and regenerate the solvent.

For both layouts, the feedstock of phenolic substrates is assumed to derive from biomass fractional pyrolysis, yielding low molecular weight phenols. The valuable end-products of the process are 2,3 dihydroxybenzoic acid (DHBA) for catechol feeding and 2,6 dihydroxy 4 methylbenzoic acid (DHMBA) for orcinol feeding.

Fig. 5 provides a detailed description of each EC reaction subunit embodying the carboxylic acids separation stage. Several separation protocols for carboxylic acids recovery after EC in highly concentrated bicarbonate solutions have been proposed in the literature to overcome EC equilibrium conversion limit (see section 1). Due to the uncertainty of the performances of immobilized DC and the lack of information about the regeneration of separating agents (resins, salts etc.), the description of the product separation process was beyond the aim of the present work. Accordingly, it was assumed that carboxylic acids could be removed entirely in the separation unit and that no product accumulation occurred in the carbonates solvent, essential to solvent regeneration/reuse.

2.2. CO_2 enzymatic reactive absorption

ASPEN PLUS® was used to model the CO_2 ERA unit. Table 1 shows the main parameters/properties of the absorption section. The flow rate and composition of the flue gas stream were set according to Russo et al. (2013b) based on a realistic case of a pilot plant (Wu et al., 2018; Smith et al., 2014). The concentration of aqueous K_2CO_3 has been fixed at 3 M, according to the literature (Matsui et al., 2006; Wuensch et al., 2014; Ren et al., 2016). The liquid-to-gas (L/G) mass ratio was increased in the two layouts until to the flooding values of 80 % given by ASPEN PLUS® corresponding to the maximum working L/G mass ratio of 5 kg/kg. The column works with negligible pressure drop for both the gas and liquid phases. The temperature of the outlet gas (Table 1) decreases as L/G ratio increases (e.g., the outlet gas is at 25.9 °C at 5 kg/kg L/G). As expected, L/G ratio has negligible effect on the temperature profile of the liquid solvent (e.g., the rich solvent is at 28.2 °C at 5 kg/kg L/G). Immobilized CA was considered confined in the absorption column, and its properties were set according to Peirce et al. (2018b), who developed a biocatalyst with CA covalently immobilized on paramagnetic nanoparticles of Fe_3O_4. The concentration of dispersed biocatalyst in the ERA unit was fixed considering a 2 %vol solid hold-up, according to Russo et al. (2016).

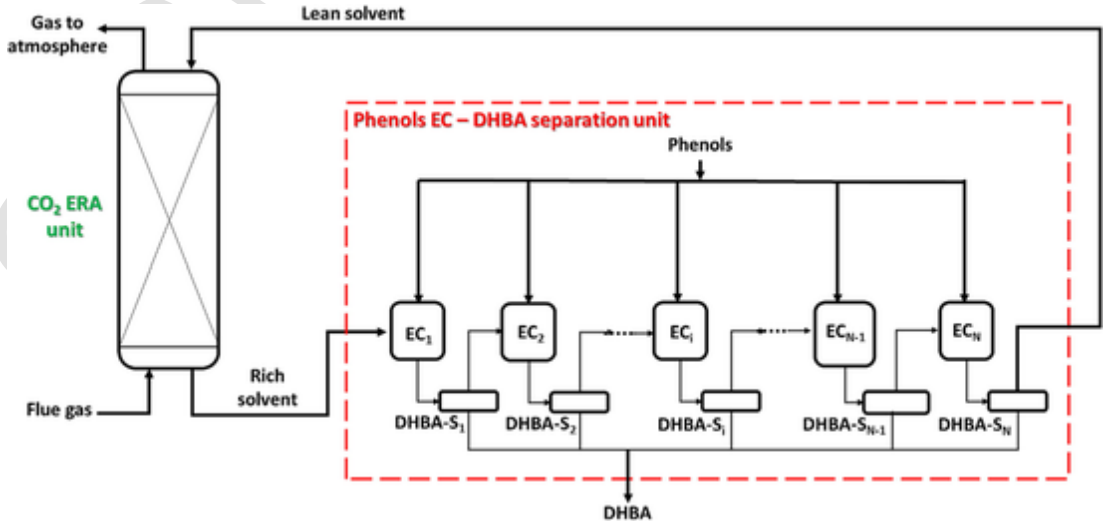

Fig. 3. Layout 1 for enzymatic CO_2 capture and carboxylation.

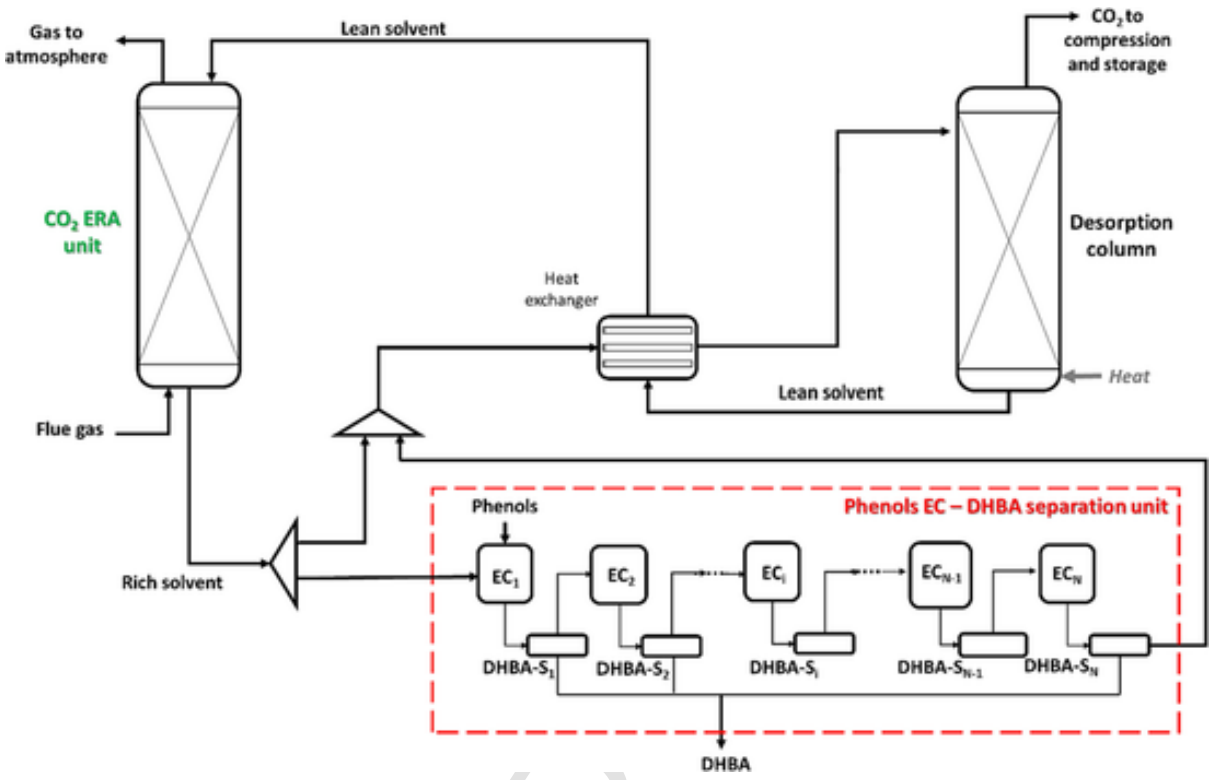

Fig. 4. Layout 2 for enzymatic CO_2 capture, storage and carboxylation.

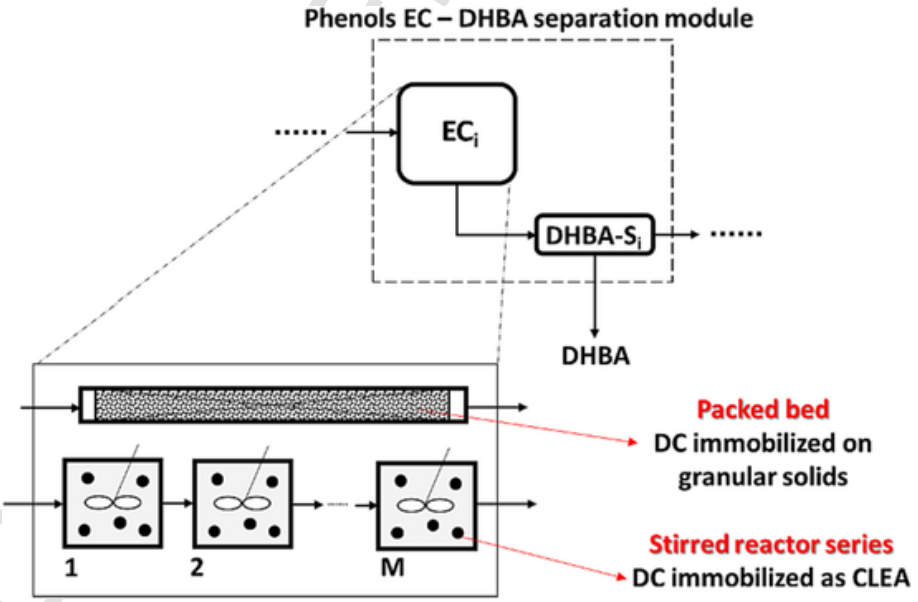

Fig. 5. EC subunits including product separation and alternative reactor configurations in the inset.

The kinetics of CO_2 hydration catalyzed by immobilized CA was reported by Peirce et al., (2018a) for experimental conditions close to those set for the ERA unit. The kinetic model of CO_2 hydration in K_2CO_3 solutions catalyzed by immobilized carbonic anhydrase was included in both forward (r_f) and backward (r_b) CO_2 hydration reactions of the ASPEN PLUS® RADFRAC column section (Eq.s 5 and 6).

$$r_f = k_E \bullet [CA]_{im} \bullet \rho_{solid} \bullet \varepsilon_s \bullet [CO_2] \quad (5)$$

$$r_b = \frac{k_E \bullet [CA]_{im} \bullet \rho_{solid} \bullet \varepsilon_s}{K_1} \bullet [HCO_3^-] \bullet [H^+] \quad (6)$$

K_1 is the CO_2 hydration reaction equilibrium constant (Eq. (1)) whose temperature dependency was calculated according to the ASPEN PLUS® properties library.

A rate-based calculation method was used to include mass transfer phenomena and CO_2 hydration kinetics, hence the effect of CA on the overall CO_2 absorption rate. ELECNRTL was used as a properties calculation model to describe electrolyte solutions.

This ERA unit design was included in both Layout 1 and Layout 2 simulations. In Layout 2, a stripping unit was also coupled to complete the absorption/desorption loop. The process flowsheet designed with ASPEN PLUS® is reported in Figure S1, and it was used to simulate the

Table 1
Main parameters of the CO_2 ERA stage.

Flue gas stream to be treated					
Flow rate	1000	Nm^3/h	N_2	0.88	mol/mol
Temperature	60	°C	H_2O	0.02	
Pressure	1.1 10^5	Pa	CO_2	0.1	
Lean solvent stream					
L/G ratio	3–5	kg/kg	Pressure	1.3 10^5	Pa
Temperature	25	°C	$[K_2CO_3]$	3	M
Biocatalyst: immobilized carbonic anhydrase					
Enzyme (CA) loading	0.04	kg/kg_{solids}	Solid hold-up	2	%vol
Solid density	5240	kg/m^3	k_E	1460	$m^3/kg\ s$
Column design					
Diameter	0.43	m	Packing type	MELLAPACK 350Y SULZER	

CO_2 absorption/desorption process in Layout 2 as an open loop to overcome any convergence issues. A RADFRAC column model was applied using the EQUILIBRIUM calculation, and simulations were carried out by setting 5 stages with a $3{\cdot}10^4$ Pa pressure at stage 1 (condenser), 70 °C rich solvent inlet temperature, and by varying the reboiler thermal duty (at stage 5) to reach a satisfactory solvent regeneration so that the solvent loading was smaller than 0.55 mol_C/mol_{K+}.

2.3. Enzymatic carboxylation

A preliminary study (Marra et al., 2022) first analyzed coupling the CO_2 ERA process with EC through an equilibrium model based on published data on reversible enzymatic carboxylation of several phenolic substrates, such as catechol and orcinol (Pesci et al., 2015; Meyer et al., 2018; Ohde et al., 2021). The present model is based on the realistic assumption that (de)carboxylases (DCs) may be immobilized to be used in a continuously operated EC reactor. Depending on the DC immobilization method, two alternative reactor configurations were considered:

a) DCs covalently attached on a solid granular support suitable for utilization in a packed bed reactor;

b) DCs immobilized through a covalent carrier-free technique (Cross-Linked Enzyme Aggregates – CLEA) that can be used as a dispersed solid biocatalyst in stirred reactors.

Due to the reversible nature of the EC reaction, the use of a segregated reactor configuration instead of a mixed type is desirable. Hence, a tubular packed bed and series of stirred reactors were considered as convenient configurations for a DC-based biocatalyst developed according to immobilization techniques a) and b), respectively. Both configurations were modelled as a series of 5 CSTR in ASPEN PLUS® using the R-CSTR module (see Fig. 5 and Figure S2).

The kinetic model of free DCs catalysis (Pesci et al., 2015) was assumed valid for the immobilized DCs and was included as a custom reaction rate equation (Eq. (7)) in ASPEN PLUS® to describe the enzymatic carboxylation of catechol.

$$r_{DHBA} = E_{load} \bullet \rho_S \bullet \frac{\varepsilon_s}{1-\varepsilon_s} \bullet \frac{\frac{V^f_{max}}{K_{mc}K^b_c} \bullet [1,2DHB] \bullet \left[HCO_3^-\right] - \frac{V^b_{max} \bullet [2,}{K_{n}}}{1 + \frac{[1,2DHB]}{K_{mc}} + \frac{[HCO_3^-]}{K_{mb}} + \frac{[2,3DHBA]}{K_{mHA}} + \frac{[1,2D}{}}$$

Eq. (7) shows the DHBA production rate where E_{load} is the immobilized DC loading (mass of immobilized enzyme per unit mass of solid support); ρ_S the solid density, ε_s volumetric hold up of solid, $V^f_{\max}$ and $V^b_{\max}$ are the maximum reaction rates for the forward and backward carboxylation reactions depending on the substrates ($[1,2DHB]$ and $\left[HCO_3^-\right]$) and the product concentration ($[2,3\,DHBA]$). Kinetic parameters in Eq. (7) were set according to Pesci et al. (2015) and reported in Table 2.

Table 2
Kinetic parameters of the reversible carboxylation of catechol catalyzed by 2,6 DHBD (Pesci et al., 2015).

Parameter	Value	Unit
V^f_{max}	2.10 10^{-5}	mol hr^{-1} mg^{-1}
V^b_{max}	6 10^{-5}	mol hr^{-1} mg^{-1}
K_{mc}	0.03	M
K^b_c	0.087	M
K_{mHA}	0.0012	M
K_{mb}	0.839	M

The properties of the biocatalysts are reported in Table 3 according to the reactor configurations described in Fig. 5. The DC loading per unit mass of solid carrier was set according to reasonable values obtained from the literature for the selected immobilization techniques. In particular, the DC loading of CLEA was set at 1000 g_E/kg_S, by assuming that the biocatalyst can be considered as a pure enzyme and neglecting the mass of the cross-linker (Peirce et al., 2017; Sheldon and Brady, 2021). Similarly, solid densities were set considering resin supports (in packed bed) and enzyme aggregates (in stirred tanks). The solid hold-up was set assuming spherically single-sized beads in the packed bed and diluted fine biocatalyst particles dispersed in the stirred tanks.

2.4. Model computation and validation methods

This section reports the description of the general model computation method and the criteria followed for model validation. The resulting data and their discussion are presented in sections 3.1-6. A base case for the simulation of the CO_2 ERA unit was established, setting the lean solvent loading at 0.5 mol_C/mol_{K+} and the 5 kg/kg L/G ratio corresponding to 80 % of the flooding limiting value ($L/G_{flooding}$ = 6.22 kg/kg). The packing height in the absorption column ranged between 3 and 10 m. The packing height with maximum CO_2 capture efficiency (Eq. (8)) was used for further sensitivity studies, where the effect of the L/G ratio and the lean solvent loading on both CO_2 capture efficiency and composition of the rich solvent was assessed.

$$CO_2\ capture\ efficiency = \frac{kg^{flue\ gas}_{CO_2} - kg^{gas\ to\ atm}_{CO_2}}{kg^{flue\ gas}_{CO_2}} \quad (8)$$

The model of the CO_2 absorption unit was validated by comparing the results of the RADFRAC model with experimental results from a pilot plant operated with no CA and a similar solvent composition (Smith et al., 2014). To this aim, the concentration of CA was set at zero, and the only CO_2 hydration and hydroxylation reactions were considered in the model. Table 4 reports experimental data (Smith et al., 2014) on the absorption column geometry, packing type, operating temperatures, and L/G ratio used for the validation.

The EC unit simulations were performed to assess its size in terms of the number and volume of modular tubular or stirred reactors with different initial conditions for both Layouts 1 and 2.

Table 3
Properties of immobilized decarboxylases.

Reactor configuration	Packed bed	Stirred reactor series
DC immobilization technique	Covalent attachment on solid particles	Cross-linked enzyme aggregates
Enzyme loading $[g_{Enz}/kg_{sol}]$	10–100	1000
Solid density $[kg_{sol}/m^3_{sol}]$	1200	1050
Solid hold-up $[m^3_{sol}/m^3_{liq}]$	0.6	0.02

Table 4
Selected parameters for the literature pilot runs used for absorption model validation (Smith et al., 2014).

L/G [kg/kg]	Gas Pressure [kPag]	Flue gas temperature [°C]	Lean solvent temperature [°C]	Lean solvent K_2CO_3 concentration [wt%]	Packing height [m]	Column Diameter [m]	Packing type
3	2	41	49	28	4.8	0.21	Sulzer Mellapak (standard)
4	5	65	41				
5	5	40	40				

In Layout 1 simulations, the minimum number of EC subunits (see Fig. 3) required to achieve the complete conversion of captured CO_2 (dissolved in the rich solvent as HCO_3^- ions according to the simulation of the CO_2 ERA unit base case) was calculated assuming that the maximum phenol carboxylation degree was obtained in each EC subunit. The composition of the outlet stream from each EC subunit was assessed by the previously developed equilibrium model (Marra et al., 2022) that provided the consumption of HCO_3^- occurring at each EC step supplied with a phenol stream at 50 and 80 mM catechol/orcinol. In Layout 1, the CO_2 ERA best case (L/G ratio and solvent loading) was selected to minimize the number of EC subunits required to fix 1 kg/h of captured CO_2.

Similar calculations were performed to assess the minimum number of modules of the EC section in Layout 2. In this case, the effect of product separation efficiency (20–100 %) on the minimum number of modules of the EC section was assessed. The mass flow of phenols available as a product of a pyrolytic bio-oil production/fractionation plant was assumed as the limiting operating parameter. Phenolic substrates can be obtained as a fraction of pyrolytic bio-oil from several biomass feedstocks (Dhyani and Bhaskar, 2018). Accordingly, phenols mass flow was estimated for a typical biomass fast pyrolysis capacity plant of 10 tons/day with a 50 % bio-oil fraction, and a 2 % low molecular weight phenols yield upon bio-oil fractionation.

The fraction of the rich solvent processed in the EC stage was set according to the solubility limit of phenols (see Fig. 2). In Layout 2, the CO_2 ERA best case was selected to maximize the CO_2 capture from flue gas by adjusting the heat input to the regeneration to reach lean solvent loading of 0.54 mol_C/mol_{K+}.

For both layouts and EC reactor configurations, the size of each EC reactor was calculated as follows. First, the volumetric concentration of immobilized DC enzymes (referred to the liquid phase) was calculated according to immobilized DC properties (Table 3). Then, the liquid-phase hydraulic residence time (HRT_{liq}) was iteratively varied in the ASPEN PLUS® R-CSTR model until the maximum equilibrium conversion was approached. The liquid volume was calculated from the HRT_{liq} taking into account the liquid flow rate as well as the total reactor volume, and considering the solid hold-up set in Table 3.

3. Results and discussion

3.1. Validation of the CO_2 absorption unit model

Despite the CA selected for the present model has been extensively characterized from the standpoint of immobilized enzyme kinetics under conditions relevant to the study (Peirce et al., 2018b), no data are available at the pilot scale. At the same time, no kinetic models are reported in the literature for other CA forms that have been successfully tested in pilot plants (Kunze et al., 2015, Reardon et al., 2014). For these reasons, the absorption unit model was validated by matching results of computations against experimental results published by Smith et al. (2014), characterized by similar solvent composition (Table 4), although no CA was used. It is reasonable to assume that the immobilized CA has a very limited impact on the vapour-liquid equilibria and chemical-physical properties of the solvent. Accordingly, this approach allowed validating the design method of the absorption column also in the case of the CA-catalyzed reaction. Fig. 6 compares the experimental data in terms of CO_2 capture efficiency corresponding to three values of L/G mass ratio with results from model computations for the set of operating parameters reported in Table 4. A fair agreement between the simulations and the experimental data is recorded. Indeed, for each L/G value, the simulation results (diamonds) are included in the range of the observed capture efficiencies (vertical bars).

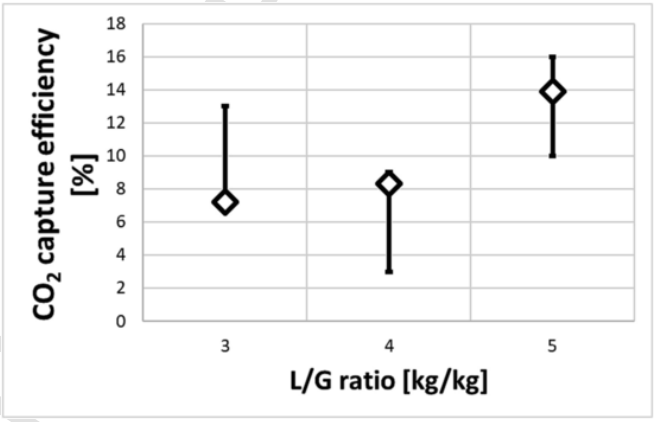

Fig. 6. Validaton of the CO_2 absorption unit submodel. Vertical bars: ranges of experimental data from Smith et al. (2014), diamonds: theoretical data according to the present study.

3.2. CO_2 enzymatic reactive absorption

Several simulations were run setting the parameters as in Table 1 to assess the effect of the packing diameter (0.43–1 m) on the performances of the column. The results are reported in Figure S3. The 0.43 m diameter was set similarly to the value reported by Smith et al. (2014) for a pilot-scale absorption column. Then, the effect of CA on the overall performance of CO_2 ERA was assessed for a 0.43 m diameter and is reported in Fig. 7 for a range of packing heights. Without CA, the CO_2 capture efficiency increases almost linearly with the packing height. In

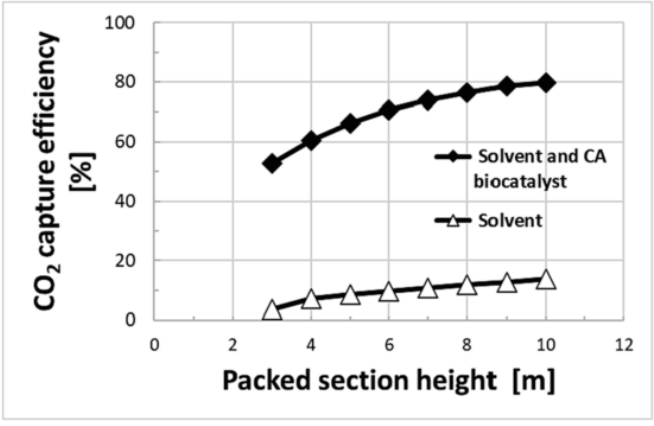

Fig. 7. Effect of packing height on CO_2 capture efficiency in CO_2 ERA unit with and without CA (operating conditions and solvents composition in Table 1).

the presence of CA immobilized on fine particles dispersed in the liquid solvent, the CO_2 capture efficiency increased from 6 to 14 times depending on the packing height. Increasing the packing height above 7 m yields a moderate growth of the CO_2 capture efficiency (<3%). Thus, the base case was selected as 7 m packing height, 4.98 kg/kg L/G ratio (80 % from flooding), and 0.5 mol_C/mol_{K+} lean solvent loading, corresponding to 74 % CO_2 capture efficiency.

3.3. Impact of lean solvent loading on capture efficiency and rich solvent composition

The performances of the ERA unit were investigated by simulations performed at lean solvent loading values ranging from 0.5 mol_C/mol_{K^+} (pure solvent) to 0.75 mol_C/mol_{K^+} to mimic a regenerated solvent with residual bicarbonate. Fig. 8 A-B report these results referred to L/G ratios ranging between 50 and 80 % of the flooding value. Larger bicarbonate concentrations reduced the CO_2 capture efficiency by decreasing the overall reaction rate and yielded larger bicarbonate concentrations in the rich solvent (up to 1.88 M). According to Marra et al. (2022), the bicarbonate concentration is crucial to select proper conditions at the inlet of the EC unit to promote the conversion of phenols via the reversible enzymatic carboxylation. This criterion and the results in Fig. 8B were considered to set the conditions for the simulations of Layout 1, as discussed in the next section.

3.4. Model computations: Layout 1

The L/G ratio and the lean solvent loading are the key variables to ensure both a satisfactory CO_2 capture efficiency and an appropriate value of bicarbonate concentration in the rich solvent. Indeed, large bicarbonate concentrations (>1M) are necessary to push the maximum theoretical limit of phenols carboxylation degree. The simulations of Layout 1 were aimed at the assessment of the required number of EC modules to achieve the complete conversion of the captured CO_2 in a range of L/G mass ratios and solvent loadings values. The overall number of EC subunits (NECS) is a function of the bicarbonate concentration in the rich solvent that, in turn, affects both the phenols conversion degree and the CO_2 capture efficiency. Moreover, NECS depends on the carboxylation equilibrium constant and thus on the type of phenolic substrate and its inlet concentration in each EC reactor. This limits the amount of CO_2 that can be fixed in each EC subunit. Indeed, each EC reactor can convert a stoichiometric amount of bicarbonate depending on

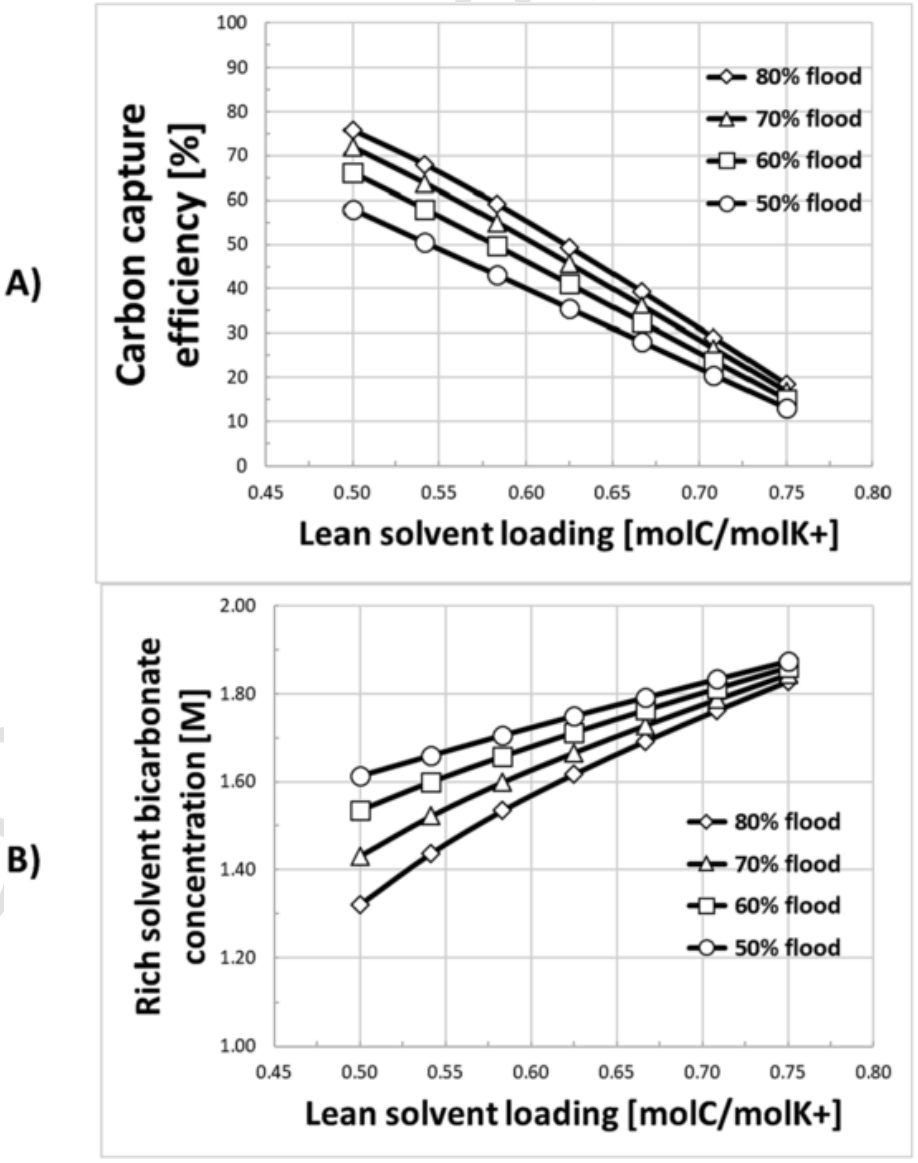

Fig. 8. Effect of the lean solvent loading on A) CO_2 capture efficiency and B) bicarbonate concentration in the rich solvent as a function of the L/G mass ratio.

the theoretical equilibrium conversion that is about 20 % and 50 % for catechol and orcinol, respectively, according to the available data on EC equilibria (Pesci et al., 2015; Meyer et al., 2018). Also, the mass flow rate of captured CO_2 decreases at increasing solvent loading and decreasing L/G ratios. The number N_{Fix} of EC subunits required to fix 1 kg/h of captured CO_2 was calculated as the ratio between NECS and the mass flow of captured CO_2 (m_{CO2}) (Eq. (9)).

$$N_{Fix} = \frac{Number\ of\ EC\ subunit\ for\ complete\ conversion\ of\ captured\ CO_2}{m_{CO_2}} \quad (9)$$

Fig. 9 shows the effect of the lean solvent loading on N_{fix}. As m_{CO2} decreased at increasing solvent loading, a smaller value of NECS is required to fully convert the captured CO_2 into carboxylic acids (Figure S4, S5). In addition, as the bicarbonate concentration in the rich solvent increased, N_{fix} decreased because of the beneficial effect of the larger bicarbonate excess on the maximum phenols carboxylation degree (see section 1).

Data in Fig. 9 show how the value of N_{Fix} decreases as the L/G ratio increases. At a given solvent loading, a negligible decrease of NECS with increasing L/G ratio is expected because the larger amount of captured CO_2 (m_{CO2}) per unit volume of liquid flow (L) (Figure S6) is damped by the larger liquid solvent flow (decrease of the bicarbonate concentration in reach solvent at increasing L/G ratios – Fig. 8B). The reduction of N_{Fix} is negligible for solvent loading larger than 0.67 mol_C/mol_{K+} at any L/G ratio. Accordingly, 0.67 mol_C/mol_{K+} was set as the optimal loading for Layout 1, and N_{Fix} was calculated for orcinol and catechol carboxylation (Fig. 10). N_{Fix} is smaller for orcinol because of the value of the carboxylation equilibrium constant (0.16 M^{-1} and 0.5 M^{-1} for orcinol and catechol respectively) and decreases at increasing inlet phenols concentration. This is related to the stoichiometric ratio between available phenols and the amount of bicarbonate fixed as carboxylic acids.

The iterative procedure described in section 1.4 was applied to assess the reactor volume of each EC subunit, assuming a packed bed and series of stirred reactors as alternative configurations. In the case of a packed bed, the DCs are immobilized in granular solids, and the reactor volume below which there is an appreciable departure from the maximum conversion of the phenolic substrate was of about 1 m^3 (Fig. 11). The calculation was repeated for several concentrations of immobilized DCs. In the absence of specific kinetic data for immobilized DC, the kinetics of immobilized DC was described starting from the parameters available for free DC (Table 2). The activity of immobilized DCs has been rated at 50 % of the free enzyme activity, as a partial deactivation of the enzyme is expected upon immobilization. As expected, the effect of the inlet catechol concentration on the reactor volume is negligible since the substrate concentration does not significantly affect the EC equilibrium conversion (Marra et al., 2022). According to the literature, 25–50 mg/g of immobilized DC per unit mass of solid support is a reasonable loading (Russo et al., 2022). This makes the prediction of EC subunits having volumes smaller than 1 m^3 reliable. Similar calculations were applied to the case of the stirred reactor series. Fig. 12 shows the overall reaction volume for each reactor configuration. The packed bed reactors require smaller volumes than the cascade of stirred reactors to approach the equilibrium conversion of catechol carboxylation. This is due to the typical solid hold-up of packed bed reactors (0.6 according to Table 3) larger than that establishing in mixed reactors (0.02). This difference impacts positively and overtakes the effect of the immobilized DC loading that ranges from 5 to 50 g/kg for packed solids to 100–500 g/kg for suspended cross-linked aggregates in the mixed reactors. In the EC section, the size of each reactor decreases along the series of subunits due to the progressing decrease of the bicarbonate concentration (e.g. from 1.69 to 1.37 M in layout 1) upon carboxylation. Because of the effect of bicarbonate on the theoretical catechol conversion degree, it drops from 21.2 to 17.9 % along the series of EC subunits.

3.5. Model computations: Layout 2

The results from the sensitivity analysis guided the selection of the input values for simulations of Layout 2. As previously discussed, Layout 2 corresponds to a general-purpose CO_2 capture plant (Table 1), whence a portion of the captured CO_2 via ERA is valorized through phenol enzymatic carboxylation. Input data for this configuration were based on typical operating conditions of such plants and are reported in

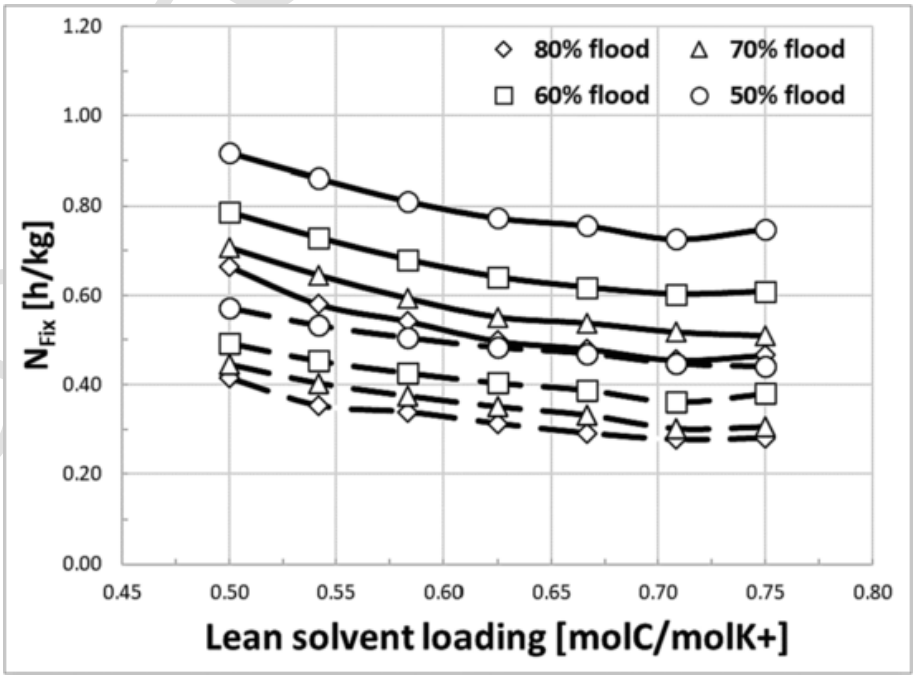

Fig. 9. Effect of the lean solvent loading on the number of EC subunits required to convert 1 kg/hr of captured CO_2 (N_{fix}), 50 mM (solid lines) and 80 mM (dashed lines) catechol concentration.

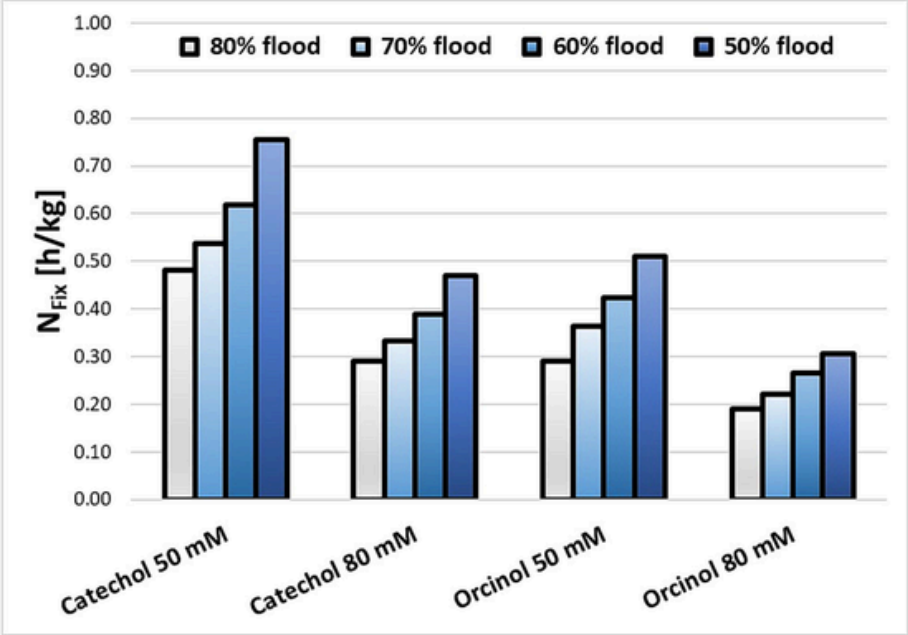

Fig. 10. Effect of the L/G mass ratio (as a fraction of flooding point) on the number of EC subunits required to convert 1 kg/hr of capture CO_2 as a function of phenolic substrate concentration (lean solvent loading 0.67 mol_C/mol_{K+}),.

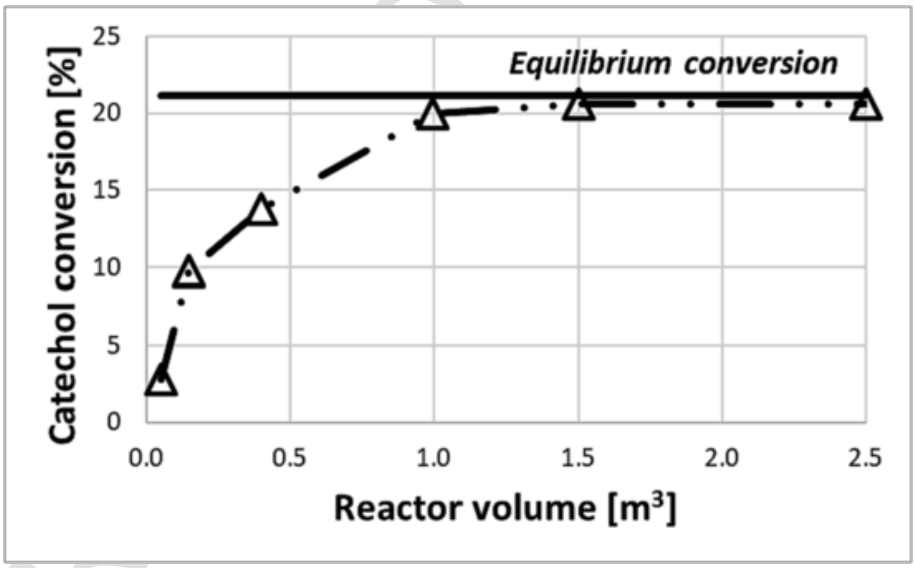

Fig. 11. Effect of the reactor volume (packed bed) on catechol conversion degree for a 25 mg/g loading of actively immobilized DC.

Table 5. In particular, maximization of the capture efficiency is typically accomplished by increasing the L/G ratio and keeping the lean solvent loading as low as possible by solvent regeneration.

The results of the CO_2 ERA model simulations are reported in Table 6. As expected, CO_2 capture efficiency (68 %) is higher than in Layout 1 (39 %). Hence, the rich solvent bicarbonate concentration is smaller due to the smaller lean solvent loading (0.54 mol_C/mol_{K^+}). With these numbers, the reboiler duty was a 5.54 MJ/kg_{CO2} (see section 2.2). In Layout 2 the mass flow of phenols was assumed as the limiting factor to the conversion of the captured CO_2. The available stream of phenols from pyrolytic bio-oil fractionation was used. The pyrolysis plant is assumed to have the capacity of 10 tons/day with a 50 % bio-oil yield and a 2 % weight fraction of low molecular weight phenols of the bio-oil. The rich solvent fraction used to feed the EC unit was calculated by the amount of the available phenol and by setting 50 – 80 mM as the inlet concentration of catechol (Table 6).

As expected, the conversion of orcinol is achieved with a smaller number of EC subunits due to the more favourable equilibrium carboxylation constant (Meyer et al., 2018). Because computations were performed with a fixed mass flow rate of phenols (4.2 kg/h), the different molecular weights of catechol and orcinol yielded a small difference between the total amounts of fixed CO_2 in the two acid products. Due to the negligible effect of the inlet phenol concentration on the theoretical maximum conversion, the number of EC subunits did not change when inlet substrate concentration ranged between 50 and 80 mM. How the inlet concentration of substrate affected the volume of EC subunits was calculated for Layout 2, assuming that the maximum catechol conversion was approached in the continuous steady operation. Results in Fig. 13 show the overall reaction volume for both biocatalyst types (Table 2): DCs attached on solid particles in a packed bed reactor or series of stirred reactors operated with dispersed cross-linked enzyme aggregates. The inlet catechol concentration affects the reactor volumes due

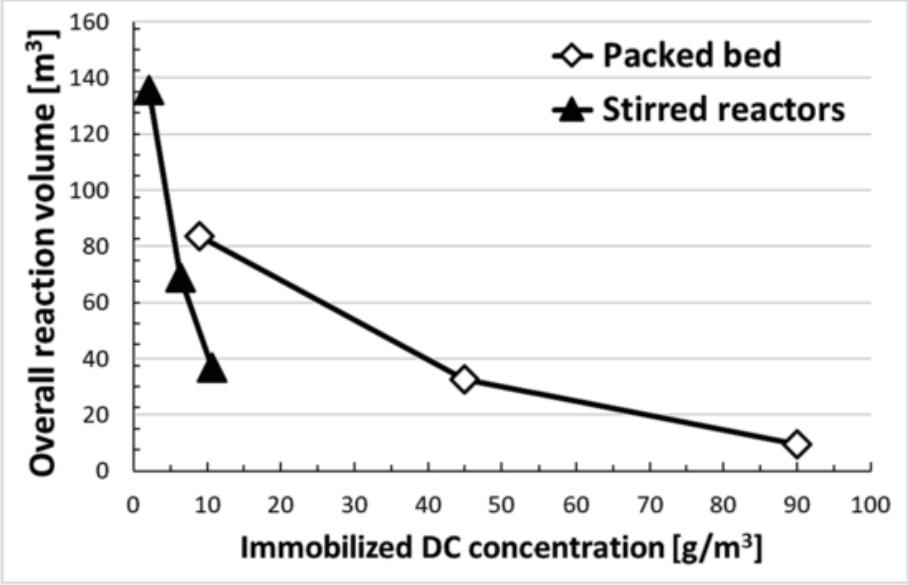

Fig. 12. Overall reaction volume of the EC section in Layout 1 as a function of the concentration of immobilized DC (referred to the liquid volume). Substrate: catechol, solvent loading = 0.67 mol_C/mol_{K+}, L/G = 80 % $L/G_{flooding}$.

Table 5
Base case operating conditions and performances of CO_2 ERA unit in Layout 2.

L/G ratio	4.98	kg/kg
Lean solvent loading	0.54	mol_C/mol_{K^+}
Packed section height	7	m
Bicarbonate in rich solvent	1.44	M

Table 6
Results of Layout 2 simulations.

Inlet phenol	Number of EC subunits	Converted Phenol [kg/h]	Converted CO_2 [kmol/h]	Rich solvent split fraction [%vol]
Catechol 50/ 80 mM	6	4.2	0.038	17.1/10.7
Orcinol 50/ 80 mM	4		0.034	15.2/9.5

to the combined effects of the reaction kinetics and of the total volumetric flow to be processed.

The effect of carboxylic acid concentration on the reaction volume was assessed assuming a separation efficiency between 20 and 100 % (Fig. 14). The conversion of catechol in each EC subunit decreases due to the accumulation of the product. The number of EC subunits (9) and the total reaction volume of the EC section (0.45 m^3 at 90 g/m^3 immobilized DC concentration, Fig. 13) are both still reasonably small at 80 % product separation efficiency.

3.6. Comparison between alternative process layouts

Table 7 reports an overview of the process variables for the two investigated Layouts, providing the starting point for an assessment and a comparison between the two options.

Layout 1 accomplishes complete fixation of the captured CO_2 without the stripping section, hence, with no recovery and storage of gas phase concentrated CO_2. The ERA section follows optimization criteria driven by the need to ensure large excess bicarbonate in the rich solvent to push the theoretical maximum conversion in the EC section of the process. The resulting operating conditions (lean solvent loading 0.67 mol_C/mol_{K+}) bring about a reduction of the CO_2 capture capacity (36 %) compared with Layout 2. The phenol throughput is 327 kg/h, a remarkably large value that implies an extensive and reliable bio-oil supply to sustain steady feeding and operation.

In Layout 2, the enzymatic carboxylation is a side process integrated into an existing ERA-based CO_2 capture plant. Only a limited fraction of the captured CO_2 is converted to valuable products via carboxylation of phenols. Simulations reported in this study refer to 4.2 kg/h phenol feeding under the hypothesis that a single medium-sized biomass pyrolysis plant could supply the required phenol feedstock. Despite this small fraction handled for CO_2 utilization purposes and its negligible impact on the reboiler heat duty, the production of value-added carboxylic acids can support the costs of the entire CCU/S process. Moreover, larger phenol feed rates might be considered, depending on the potential of the bio-oil supply chain and on economic optimization criteria. Increasing the phenol throughput according to the proposed scheme could be accomplished by adjusting the rich solvent split fraction, that is, increasing the rich solvent feed rate to the EC section so as to keep phenol concentration in the EC feeding within the solubility limit. The maximum theoretical carboxylation potential would correspond to 100 % rich solvent processed in the EC section (4.45 m^3/h), which would bear a maximum mass flow rate of dissolved catechol equal to 24.5 kg/h. This is much less than the phenol throughput of Layout 1. It is worth noting, however, that the throughput of Layout 2 might be further increased beyond this limit by implementing the distributed phenol feeding pattern that was assumed in Layout 1: phenols are fed as parallel streams to each EC subunit so as to keep the phenol concentration in each subunit below the solubility limit.

Altogether, Layout 1 may be considered a benchmark, a solution aiming at the very ambitious target of accomplishing complete fixation of captured CO_2, a potential candidate for dedicated production of added value CO_2-based chemicals when the CCU concept must be emphasized over CCS. The inherent advantage of the lack of the CO_2 stripping section and the larger throughput is counterbalanced by the smaller CO_2 capture efficiency and some lack of process flexibility, especially with respect to the reliability of the phenol supply. Conversely, Layout 2 is inherently more robust and flexible and can be retrofitted to an existing CO_2 capture plant, provided that bicarbonate solutions are produced as the intermediate carbon vector. The process robustness is

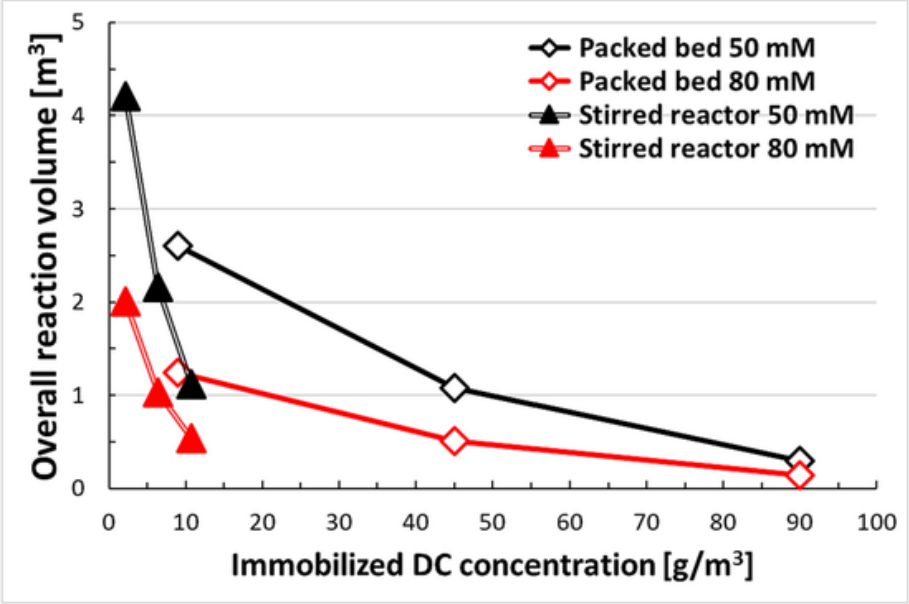

Fig. 13. Overall reaction volume of EC section in Layout 2 as a function of the concentration of immobilized DC (referred to liquid volume). Substrate: catechol; solvent loading = 0.54 mol $_{C}$/mol$_{K+}$, L/G = 80 % L/G$_{flooding}$.

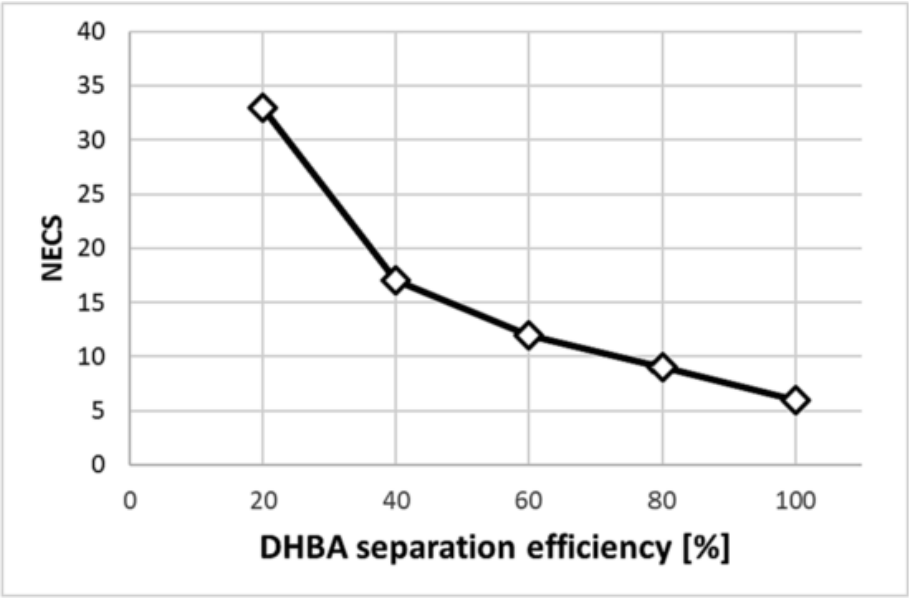

Fig. 14. Number of EC subunits required to achieve complete conversion of catechol (50 mM) in Layout 2 as a function of DHBA separation efficiency.

essentially warranted by the stripping section, which provides a stable and reliable backup to compensate for any variability of bio-oil supply and performance of the EC section.

4. Conclusions

The production of valuable dihydroxybenzoic acids by phenol carboxylation has been assessed through a system design study. Using biobased phenols derived from fast pyrolysis of biomass as the carboxylation substrates establishes an attractive bridge between bioprocess engineering and thermochemical conversion of biomass. Phenol carboxylation is accomplished via enzyme-catalyzed reaction of the phenolic substrate with a bicarbonate-rich aqueous stream coming from the carbonic anhydrase-catalyzed reaction/absorption of CO_2 from concentrated sources (e.g. flue gases). Two alternative process layouts have been simulated using the ASPEN PLUS® process simulator, using kinetic data for the biocatalytic steps (CA-promoted CO_2 capture and DC-catalyzed phenols carboxylation) obtained from dedicated experiments and from the literature. Both layouts are examples of "direct" CO_2 utilization in an aqueous phase catalyzed by enzymes.

Layout 1 assumes a scenario of complete fixation of CO_2 into dihydroxybenzoic acids, with a dedicated CO_2 capture plant and a phenolic compounds supply chain consistent with a vision based on decentralized pyrolysis of raw biomass and generation of bio-oil that feeds into centralized biorefineries. The optimization of CO_2 ERA operating conditions makes the capture and fixation of CO_2 into valuable bio-based products feasible with no need for thermal regeneration of the liquid solvent. This ambitious target is pursued at the expense of reducing the CO_2 absorption capacity with respect to conventional CCS processes.

Table 7
Comparison between Layout 1 and Layout 2.

EC substrate		Catechol		Orcinol	
Process layout		Layout 1	Layout 2	Layout 1	Layout 2
INPUT VARIABLES	Phenol feeding mass flow rate [kg/h]	327	4.82	327	4.82
	Optimal lean solvent loading [mol $_C$/mol $_{K+}$]	0.67	0.54	0.67	0.54
	phenol concentration in EC feeding [mM]	50/80			
	L/G optimal ratio [kg/kg]	4.98 (80 % of flooding point)			
OUTPUT VARIABLES	Carboxylic acid produced [kg/h]	509	6.5	550	6.3
	CO_2 ERA capture efficiency [%]	36	64	36	64
	Number of EC subunits	33/20	6	20/13	4
	Overall reaction volume[(a)] [m^3]	32.6/ 19.8	1.07/ 0.51	–	
	Overall fixed CO_2 [%]	36	0.82	36	0.73

(a) only the option of packed bed reactors is reported, assuming 25 g/kg immobilized enzyme loading.

A second scenario (Layout 2) assumes a CO_2 ERA-based closed-loop process, whence a fraction of the bicarbonate intermediate is used for carboxylation of pyrolytic phenols. The maximum fractional amount of CO_2 fixed as carboxylic acids is smaller and is limited by phenol solubility in the rich solvent. Layout 2 is inherently more flexible, thanks to the presence of the CO_2 stripping section, and may be implemented as a retrofitting of an existing capture plant.

The two layouts are representative of different realistic contexts and are characterized by different optimization criteria. Both deserve consideration for future developments aimed at exploiting biogenic resources in combination with CO_2 capture and utilization. Results of model computations provide guidelines for developing decarboxylases-based biocatalysts and for designing multiphase EC bioreactors. Moreover, they pinpoint research priorities and further steps that may support process development:

- testing pyrolytic phenols (or mixtures thereof) as sources of electron-rich substrates for EC;
- developing robust and efficient immobilization techniques to stabilize (de)carboxylases in continuous-flow reactors;
- extend the design study to the integration of continuous *in-situ* product separation with EC reactors.

Declaration of competing interest

The authors declare that they have no known competing financial interests or personal relationships that could have appeared to influence the work reported in this paper.

Data availability

Data will be made available on request.

Acknowledgements

The study has been funded under the Italian National Recovery and Resilience Plan (NRRP), Mission 4 Component 2 Investment 1.3 - Call for tender No. 1561 of 11.10.2022 of *Ministero dell'Università e della Ricerca* (MUR) funded by the European Union – NextGenerationEU; Project code PE0000021, Concession Decree No. 1561 of 11.10.2022 adopted by *Ministero dell'Università e della Ricerca* (MUR), Project title "Network 4 Energy Sustainable Transition – NEST"

Appendix A. Supplementary data

Supplementary data to this article can be found online at https://doi.org/10.1016/j.ces.2023.119618.

References

Aresta, M., Quaranta, E., Liberio, R., Dileo, C., Tommasi, I., 1998. Enzymatic synthesis of 4-OH-benzoic acid from phenol and CO_2: The first example of a biotechnological application of a carboxylase enzyme. Tetrahedron 54 (30), 8841–8846. https://doi.org/10.1016/S0040-4020(98)00475-X.

Borhani, T.N.G., Azarpour, A., Akbari, V., Wan Alwi, S.R., Manan, Z.A., 2015. CO_2 capture with potassium carbonate solutions: a state-of-the-art review. International Journal of Greenhouse Gas Control 41, 142–162. https://doi.org/10.1016/j.ijggc.2015.06.026.

Brown, R.C., 2021. Heterodoxy in fast pyrolysis of biomass. Energy & Fuel 35 (2), 987–1010. https://doi.org/10.1021/acs.energyfuels.0c03512.

Comstock, C., Dodge, B., 1937. Rate of carbon dioxide absorption by carbonate solutions in a packed tower. Industrial & Engineering Chemistry 29 (5), 520–529.

De Carvalho Pinto, P.C., Batista, T.V., De Rezende Ferreira, G., Voga, G.P., Oliveira, L.C.A., Oliveira, H.S., De Souza, L.A., Belchior, J.C., 2022. Chemical absorption of CO_2 enhanced by solutions of alkali hydroxides and alkoxides at room temperature. Chemistry Select 7 (43). https://doi.org/10.1002/slct.202202731.

Dhyani, V., Bhaskar, T., 2018. A comprehensive review on the pyrolysis of lignocellulosic biomass. Renewable Energy 129, 695–716. https://doi.org/10.1016/j.renene.2017.04.035.

Dineshkumar, R., Dash, S.K., Sen, R., 2015. Process integration for microalgal lutein and biodiesel production with concomitant flue gas CO_2 sequestration: a biorefinery model for healthcare, energy and environment. RSC Advances 5 (90), 73381–73394. https://doi.org/10.1039/c5ra09306f.

Ember, 2022. Last access: March 2023. Clim. Change. https://ember-climate.org/data/data-tools/carbon-price-viewer.

Fonts, I., Atienza-Martínez, M., Carstensen, H.H., Benés, M., Pires, P.P., 2021. Thermodynamic and physical property estimation of compounds derived from the fast pyrolysis of lignocellulosic materials. Energy & Fuel 35 (21), 17114–17137. https://doi.org/10.1021/acs.energyfuels.1c01709.

Glueck, S.M., Gömös, S., Fabian, W.M.F., Faber, K., 2010. Biocatalytic carboxylation. Chemical Society Reviewes 39 (1), 313–328. https://doi.org/10.1039/b807875k.

Harte, C., Baker, E., 1933. Absorption of carbon dioxide in sodium carbonate-bicarbonate solution, II. Rate of absoprtion. Industrial & Engineering Chemistry 25 (10), 1128–1132.

He, N., Chen, Q., Fan, J., Song, F., Zhang, Y., Mu, H., 2023. Comprehensive exploration of the adsorption capacity of innovative betaine-based deep eutectic solvents for carbon dioxide capture. Journal of Chemical Thermodynamics 178. https://doi.org/10.1016/j.jct.2022.106958.

Hizaddin, H.F., Wazeer, I., Huzaimi, N.A.M., El Blidi, L., Hashim, M.A., Lévêque, J.M., Hadj-Kali, M.K., 2022. Extraction of phenolic compound from model pyrolysis oil using deep eutectic solvents: computational screening and experimental validation. Separations 9 (11). https://doi.org/10.3390/separations9110336.

Hu, G., Nicholas, N.J., Smith, K.H., Mumford, K.A., Kentish, S.E., Stevens, G.W., 2016. Carbon dioxide absorption into promoted potassium carbonate solutions: a review. International Journal of Greenhouse Gas Control 53, 28–40. https://doi.org/10.1016/j.ijggc.2016.07.020.

Jun, S.H., Yang, J., Jeon, H., Kim, H.S., Pack, S.P., Jin, E., Kim, J., 2020. Stabilized and immobilized carbonic anhydrase on electrospun nanofibers for enzymatic CO_2 conversion and utilization in expedited microalgal growth. Environmental Science & Technology 54 (2), 1223–1231. https://doi.org/10.1021/acs.est.9b05284.

Kang, K., Klinghoffer, N.B., El Ghamrawy, I., Berruti, F., 2021. Thermochemical conversion of agroforestry biomass and solid waste using decentralized and mobile systems for renewable energy and products. Renewable and Sustainable Energy Reviews 149, 111372. https://doi.org/10.1016/j.rser.2021.111372.

Knuutila, H., Svendsen, H.F., Anttila, M., 2009. CO_2 capture from coal-fired power plants based on sodium carbonate slurry; a systems feasibility and sensitivity study. International Journal of Greenhouse Gas Control 3 (2), 143–151. https://doi.org/10.1016/j.ijggc.2008.06.006.

Knuutila, H., Juliussen, O., Svendsen, H.F., 2010. Kinetics of the reaction of carbon dioxide with aqueous sodium and potassium carbonate solutions. Chemical Engineering Science 65 (23), 6077–6088. https://doi.org/10.1016/j.ces.2010.07.018.

Kunze, A., Dojchinov, G., Haritos, V.S., Lutze, P., 2015. Reactive absorption of CO_2 into enzyme accelerated solvents: from laboratory to pilot scale. Applied Energy 156, 676–685. https://doi.org/10.1016/j.apenergy.2015.07.033.

Lindsey, A.S., Jeskey, A., 1957. The Kolbe-Schmitt reaction. Journal of the Chemical Society 57, 583–620.

Liu, M., Asgar, H., Seifert, S., Gadikota, G., 2020. Novel aqueous amine looping approach for the direct capture, conversion and storage of CO_2 to produce magnesium carbonate. Sustainable Energy & Fuels 4 (3), 1265–1275. https://doi.org/10.1039/c9se00316a.

Liu, Q., Chapman, J., Huang, A., Williams, K.C., Wagner, A., Garapati, N., Sierros, K.A., Dinu, C.Z., 2018. User-tailored metal-organic frameworks as supports for carbonic anhydrase. ACS Applied Materials & Interfaces 10 (48), 41326–41337. https://

doi.org/10.1021/acsami.8b14125.
Luque, L., Westerhof, R., Van Rossum, G., Oudenhoven, S., Kersten, S., Berruti, F., Rehmann, L., 2014. Pyrolysis based bio-refinery for the production of bioethanol from demineralized ligno-cellulosic. Biomass and Bioresource Technology 161, 20–28. https://doi.org/10.1016/j.biortech.2014.03.009.
Marra, L., Knuutila, H., Russo, M.E., 2022. A novel CO_2 capture and utilization strategy by enzyme catalysis: preliminary assessment of process layout. Chemical Engineering Transactions 93, 31–36. https://doi.org/10.3303/CET2293006.
Matsui, T., Yoshida, T., Yoshimura, T., Nagasawa, T., 2006. Regioselective carboxylation of 1,3-dihydroxybenzene by 2,6-dihydroxybenzoate decarboxylase of Pandoraea sp. 12B–2. Applied Microbiology & Biotechnology 73, 95–102. https://doi.org/10.1007/s00253-006-0437-z.
Meyer, L.E., Plasch, K., Kragl, U., Von Langermann, J., 2018. Adsorbent-based downstream-processing of the decarboxylase-based synthesis of 2,6-dihydroxy-4-methylbenzoic acid. Organic Process Research & Development 22 (8), 963–970. https://doi.org/10.1021/acs.oprd.8b00104.
Ohde, D., Thomas, B., Bubenheim, P., Liese, A., 2021. Enhanced CO_2 fixation in the biocatalytic carboxylation of resorcinol: utilization of amines for amine scrubbing and in situ product precipitation. Biochemical Engineering Journal 166. https://doi.org/10.1016/j.bej.2020.107825.
Payer, S.E., Faber, K., Glueck, S.M., 2019. Non-oxidative enzymatic (De)carboxylation of (hetero)aromatics and acrylic acid derivatives. Advanced Synthesis & Catalysis 361, 2402–2420. https://doi.org/10.1002/adsc.201900275.
Peirce, S., Russo, M.E., Isticato, R., Lafuente, R.F., Salatino, P., Marzocchella, A., 2017. Structure and activity of magnetic cross-linked enzyme aggregates of bovine carbonic anhydrase as promoters of enzymatic CO_2 capture. Biochemical Engineering Journal 127, 188–195. https://doi.org/10.1016/j.bej.2017.08.014.
Peirce, S., Perfetto, R., Russo, M.E., Capasso, C., Rossi, M., Salatino, P., Marzocchella, A., 2018a. Characterization of technical grade carbonic anhydrase as biocatalyst for CO_2 capture in potassium carbonate solutions. Greenhouse Gases Sci. Technol. 8 (2), 279–291. https://doi.org/10.1002/ghg.1738.
Peirce, S., Russo, M.E., Perfetto, R., Capasso, C., Rossi, M., Fernandez-Lafuente, R., Salatino, P., Marzocchella, A., 2018b. Kinetic characterization of carbonic anhydrase immobilized on magnetic nanoparticles as biocatalyst for CO_2 capture. Biochem. Eng. J. 138, 1–11. https://doi.org/10.1016/j.bej.2018.06.017.
Pesci, L., Glueck, S.M., Gurikov, P., Smirnova, I., Faber, K., Liese, A., 2015. Biocatalytic carboxylation of phenol derivatives: kinetics and thermodynamics of the biological Kolbe-Schmitt synthesis. FEBS Journal. 282 (7), 1334–1345. https://doi.org/10.1111/febs.13225.
Rasouli, H., Iliuta, I., Bougie, F., Garnier, A., Iliuta, M.C., 2021. Enzyme-immobilized flat-sheet membrane contactor for green carbon capture. Chemical Engineering Journal 421 (P1), 129587. https://doi.org/10.1016/j.cej.2021.129587.
Reardon, J., Bucholz, T., Hulvey, M., Tuttle, J., Shaffer, A., Pulvirenti, D., Weber, L., Killian, K., Zaks, A., 2014. Low energy CO_2 capture enabled by biocatalyst delivery system. Energy Procedia 63, 301–321. https://doi.org/10.1016/j.egypro.2014.11.033.
Ren, J., Yao, P., Yu, S., Dong, W., Chen, Q., Feng, J., Wu, Q., Zhu, D., 2016. An unprecedented effective enzymatic carboxylation of phenols. ACS Catalysis 6 (2), 564–567. https://doi.org/10.1021/acscatal.5b02529.
Russo, M.E., Olivieri, G., Capasso, C., De Luca, V., Marzocchella, A., Salatino, P., Rossi, M., 2013a. Kinetic study of a novel thermo-stable α-carbonic anhydrase for biomimetic CO_2 capture. Enzyme Microb. Technol. 53 (2013), 271–277. https://doi.org/10.1016/j.enzmictec.2013.05.002.
Russo, M.E., Olivieri, G., Salatino, P., Marzocchella, A., 2013b. CO_2 capture by biometic absorption: enzyme mediated CO_2 absorption for post-combustion carbon sequestration and storage. Environ. Eng. Manag. J. 12 (8), 1595–1603.
Russo, M.E., Bareschino, P., Olivieri, G., Chirone, R., Salatino, P., Marzocchella, A., 2016. Modeling of slurry staged bubble column for biomimetic CO_2 capture. International Journal of Greenhouse Gas Control 47, 200–209. https://doi.org/10.1016/j.ijggc.2016.01.045.
Russo, M.E., Capasso, C., Marzocchella, A., Salatino, P., 2022. Immobilization of carbonic anhydrase for CO_2 capture and utilization. Applied Microbiology & Biotechnology. https://doi.org/10.1007/s00253-022-11937-8.
Sarmad, S., Mikkola, J.P., Ji, X., 2017. Carbon dioxide capture with ionic liquids and deep eutectic solvents: a new generation of sorbents. ChemSusChem 10 (2), 324–352. https://doi.org/10.1002/cssc.201600987.
Severo, I.A., Siqueira, S.F., Deprá, M.C., Maroneze, M.M., Zepka, L.Q., Jacob-Lopes, E., 2019. Biodiesel facilities: What can we address to make biorefineries commercially competitive? Renewable and Sustainable Energy Reviews 112, 686–705. https://doi.org/10.1016/j.rser.2019.06.020.
Shamna, I., Kwan Jeong, S., Margandan, B., 2021. Covalent immobilization of carbonic anhydrase on amine functionalized alumino-Siloxane aerogel beads for biomimetic sequestration of CO_2. Journal of Industrial and Engineering Chemistry 100, 288–295. https://doi.org/10.1016/j.jiec.2021.05.010.
Sheldon, R.A., Brady, D., 2021. Streamlining design, engineering, and applications of enzymes for sustainable biocatalysis. ACS Sustainable Chemistry & Engineering 9 (24), 8032–8052. https://doi.org/10.1021/acssuschemeng.1c01742.
Smith, K., Xiao, G., Mumford, K., Gouw, J., Indrawan, I., Thanumurthy, N., Quyn, D., Cuthbertson, R., Rayer, A., Nicholas, N., Lee, A., Da Silva, G., Kentish, S., Harkin, T., Qader, A., Anderson, C., Hooper, B., Stevens, G., 2014. Demonstration of a concentrated potassium carbonate process for CO_2 capture. Energy & Fuel 28 (1), 299–306. https://doi.org/10.1021/ef4014746.
Song, C., Liu, Q., Qi, Y., Chen, G., Song, Y., Kansha, Y., Kitamura, Y., 2019. Absorption-microalgae hybrid CO_2 capture and biotransformation strategy—a review. International Journal of Greenhouse Gas Control 88, 109–117. https://doi.org/10.1016/j.ijggc.2019.06.002.
Tommasi, I.C., 2019. Carboxylation of hydroxyaromatic compounds with HCO_3^- by enzyme catalysis: recent advances open the perspective for valorization of lignin-derived aromatics. Catalysts 9 (1). https://doi.org/10.3390/catal9010037.
Troiano, M., Ianzito, V., Solimene, R., Ganda, E.T., Salatino, P., 2022. Fluidized bed pyrolysis of biomass: a model-based assessment of the relevance of heterogeneous secondary reactions and char loading. Energy & Fuels 36 (17), 9660–9671. https://doi.org/10.1021/acs.energyfuels.2c01483.
Wang, K., Zhu, G., Feng, Q., Li, X., Lv, Y., Zhao, Y., Pan, H., 2023. Influence of applied voltage on bioelectrochemical enhancement of biomethanation for low-rank coal and microbial community distribution. Bioresource Technology 369. https://doi.org/10.1016/j.biortech.2022.128466.
Wu, Y., Wu, F., Hu, G., Mirza, N.R., Stevens, G.W., Mumford, K.A., 2018. Modelling of a post-combustion carbon dioxide capture absorber using potassium carbonate solvent in Aspen Custom Modeller. Chinese Journal of Chemical Engineering 26 (11), 2327–2336. https://doi.org/10.1016/j.cjche.2018.06.005.
Wuensch, C., Gross, J., Steinkellner, G., Lyskowski, A., Gruber, K., Glueck, S.M., Faber, K., 2014. Regioselective ortho-carboxylation of phenols catalyzed by benzoic acid decarboxylases: a biocatalytic equivalent to the Kolbe-Schmitt reaction. RSC Advances 4 (19), 9673–9679. https://doi.org/10.1039/c3ra47719c.
Xu, X., Kentish, S.E., Martin, G.J.O., 2021. Direct air capture of CO_2 by microalgae with buoyant beads encapsulating carbonic anhydrase. ACS Sustainable Chemistry and Engineering 9 (29), 9698–9706. https://doi.org/10.1021/acssuschemeng.1c01618.
Yoshida, M., Fukuhara, N., Oikawa, T., 2004. Thermophilic, reversible γ-resorcylate decarboxylase from Rhizobium sp. strain MTP-10005: purification, molecular characterization, and expression. Journal of Bacteriology 186 (20), 6855–6863. https://doi.org/10.1128/JB.186.20.6855-6863.2004.